DE GRUYTER OPEN

Journal of ELECTRICAL ENGINEERING, VOL 67 (2016), NO5, 323–333

ANALYSIS AND SIMULATION ON THE EFFECT OF ROTOR INTERTURN SHORT CIRCUIT ON MAGNETIC FLUX DENSITY OF TURBO–GENERATOR

Yu-Ling He — Meng-Qiang Ke — Gui-Ji Tang — Hong-Chun Jiang — Xing-Hua Yuan *

The intent of this paper is to investigate the effect of the interturn short circuit fault (ISCF) in rotor on the magnetic flux density (MFD) of turbo-generator. Different from other studies, this work not only pays attention to the influence of the faulty degrees on the general magnetic field, but also investigates the effect of the short circuit positions on the harmonic components of MFD. The theoretical analysis and the digital simulation through the FEM software Ansoft are performed for a QSFN-600-2YHG turbo-generator. Several significant formulas and conclusions drawn from the analysis and the simulation results are obtained to indicate the relation between the harmonic amplitude of the MFD and the faulty degree (via n_m, the number of the short circuit turns), and the relation between the MFD harmonic amplitude and the faulty position (via α_r, the angle of the two slots in which the interturn short circuit occurs). Also, the developing tendency of the general magnetic field intensity, the distribution of the magnetic flux lines, and the peak-to-peak value of MFD are presented.

K e y w o r d s: turbo-generator, rotor inter-turn short circuit, faulty degree, short circuit position, MFD

1 INTRODUCTION

Over the years, the rotor interturn short circuit fault (ISCF) in generator has attracted a lot of attention. By far, people have studied the theoretical deduction and the simulation analysis of ISCF in wind powered generator [1, 2], and the change rate of the magnetic flux is analyzed as well in order to detect this fault [3]. It is found that the induced voltage in rotor can be used to predict the location and the number of short circuit turns [4]. Meanwhile, researchers have also studied the characteristics of the excitation currents [5, 6], the copper losses [5], and the unbalanced magnetic pull (UMP) for the ISCF monitoring [7–9]. Generally, at present, the application of search coils, which is mainly based on the magnetic field density (MFD) variation, is still adopted as a primary approach to monitor and diagnose this fault [10–12]. Therefore, further investigation on the MFD variety characteristics at great length is of significance and will be the key technology to improve the monitoring level on the very failure. It is shown that some specific harmonic characteristics are very helpful and even more effective than other traditional means to diagnose the fault [13, 14].

However, though the outstanding works above have obtained many significant discoveries and laid a strong foundation for the detection of ISCF, few of them have studied the detailed harmonic changing characteristics of MFD for rotor ISCF. Moreover, most of them only consider the effect of the faulty degree on the interested parameters such as the change of the induced voltage, the excitation current, the stator phase current, *etc*, while the influence of the faulty position on the magnetic parameters is rarely taken into account.

In fact, besides the interturn short circuit degree, the shorted position is also sensitive for the monitoring parameters, and even some of the primary parameters are bound up with the harmonic components of MFD. For example, the UMP, which brought in vibrations to the stator and rotor, are in proportion to the square of MFD. Therefore, it is significant to study on the detailed developing tendency and the variety regularity of the MFD components.

The intent of this paper is to find out some useful conclusions about the MFD harmonics under the ISCF, such as the developing trend of the harmonic amplitudes, and the effect of the short circuit degrees and the short circuit positions on the MFD harmonics.

2 THEORETICAL ANALYSIS

2.1 MFD in normal condition

Normally, the air gap magnetic field is of symmetric distribution, and the MFD can be written as

$$B = f(\alpha_m, t)\Lambda_0 \tag{1}$$

where a_m is the angle to indicate the circumferential position of the air-gap, Λ_0 is the permeance per unit area (PPUA), and $f(\alpha_m, t)$ is an angle and time dependent function to indicate the air gap magneto-motive force (MMF), which can be shown as Fig. 1.

* School of Energy, Power and Mechanical Engineering, North China Electric Power University, Baoding, Hebei, PR China, Corresponding author: Yu-Ling He, heyuling1@163.com

DOI: 10.1515/jee-2016-0047, Print (till 2015) ISSN 1335-3632, On-line ISSN 1339-309X

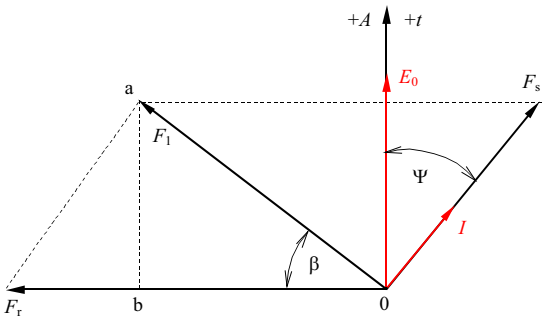

Fig. 1. MMFs under normal condition where F_s is the 1st harmonic MMF produced by armature windings, F_r is the 1st harmonic MMF produced by exciting windings, F_1 is the vector summation of F_s and F_r, Ψ is the internal power-angle of generator, function of load, I is the armature current, and E_0 is the rotor electromotive force

It is known that the exciting current, which is a DC wave, only produces odd magnetic harmonics in normal condition. Since the higher harmonics can be neglected due to their tiny values, the MMF can be described by

$$f(\alpha_m, t) = F_s \cos\big(\omega t - \alpha_m - \psi - \frac{\pi}{2}\big) + F_r \cos(\omega t - \alpha_m) = F_1 \cos(\omega t - \alpha_m - \beta) \quad (2)$$

with

$$F_1 = \sqrt{F_s^2 \cos^2\psi + (F_r - F_s \sin\psi)^2}$$
$$\beta = \operatorname{arctg} \frac{F_s \cos\psi}{F_r - F_s \sin\psi} \quad (3)$$

Then, the MFD can be given by

$$B(\alpha_m, t) = f(\alpha_m, t)\Lambda = F_1 \cos(\omega t - \alpha_m - \beta)\Lambda_0 . \quad (4)$$

According to (4), the MFD is mainly composed of the 1st harmonic component. Taking the higher order harmonics into account, there will be some odd harmonic components existing as well.

2.2 MFD under ISCF

The ISCF affects the MFD mainly by acting on the MMF. when the fault occurs, there will be an extra reverse MMF adding to the normal one, as shown in Fig. 2, where θ_r is the circumferential angle on the rotor surface, α_r is the angle between the two slots where the short circuit takes place (it is in the range of $(0, \pi)$, β' is the position angle where the short circuit begins, I_f is the exciting current, and n_m is the number of the short circuit turns.

Based on the magnetic flux conservation principle, the reverse MMF can be expressed as

$$F_d(\theta_r) = \begin{cases} -\frac{I_f n_m (2\pi - \alpha_r)}{2\pi}, & \beta' \le \theta_r \le \beta' + \alpha_r , \\ \frac{I_f n_m \alpha_r}{2\pi}, & \text{other conditions} \end{cases} \quad (5)$$

Where $F_d(\theta_r)$ can be expanded by Fourier series as

$$F_d(\theta_r) = a_0 + \sum_{n=1}^{\infty} [a_n \cos(n\theta_r) + b_n \sin(n\theta_r)] \quad (6)$$

with

$$a_0 = \frac{1}{2\pi}\int_0^{2\pi} F_d(\theta_r)\mathrm{d}\theta_r = 0 ,$$
$$a_n = \frac{1}{\pi}\int_0^{2\pi} F_d(\theta_r)\cos(n\theta_r)\mathrm{d}\theta_r = -\frac{I_f n_m[\sin(n(\alpha_r + \beta')) - \sin(n\beta')]}{n\pi} , \quad (7)$$
$$b_n = \frac{1}{\pi}\int_0^{2\pi} F_d(\theta_r)\sin(n\theta_r)\mathrm{d}\theta_r = \frac{I_f n_m[\cos(n(\alpha_r + \beta')) - \cos(n\beta')]}{n\pi} .$$

As a result, the distribution of the magnetic flux lines will have a distortion, as indicated in Fig. 3. Normally, the magnetic neutral line is in accordance with the section axis of the rotor, and the magnetic flux lines of the N-pole and the S-pole are symmetrically distributed about the neutral line. However, when the ISCF takes place, the neutral line will be shifted away from the shorted side. The more turns are shorted, the larger the shifted angle φ will be. Besides, the magnetic flux lines will be sparser on the shorted side, and $B_N(\pi+2\varphi) = B_S(\pi-2\varphi)$, where B_N and B_S are the MFD of the N-pole and the S-pole, respectively.

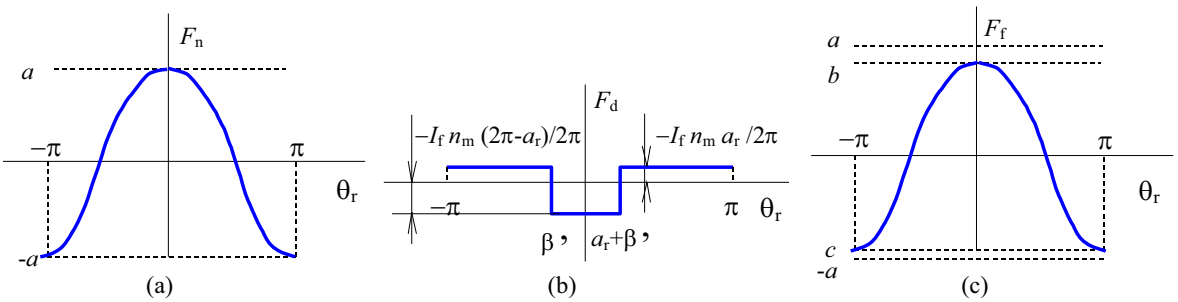

Fig. 2. MMFs under normal condition and ISCF: (a) — MMF in normal condition, (b) — the reverse MMF produced by the short-circuit turns, and (c) — the composite MMF under ISCF

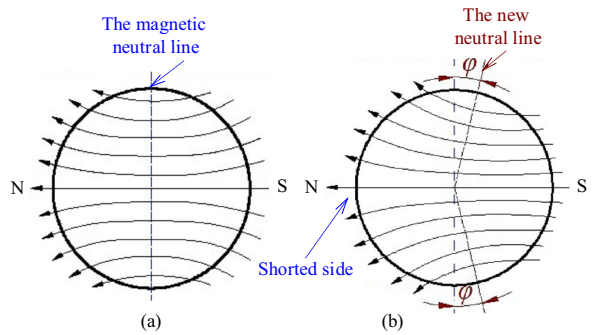

Fig. 3. Distribution of magnetic flux lines: (a) — normal, and (b) — ISCF

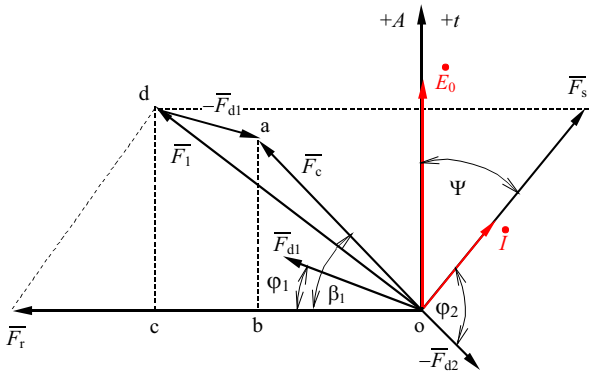

Fig. 4. MMF under ISCF

Table 1. Values of α_r when F_{dn} is zero

Harmonic order numbers	Value of α_r
$n = 1$	None
$n = 2$	None
$n = 3$	$2\pi/3$
$n = 4$	$\pi/2$
$n = 5$	$2\pi/5,\ 4\pi/5$
$n = 6$	$\pi/3,\ 2\pi/3$
$\vdots$	$\vdots$

As a result, $F_d(\theta_r)$ reduces to

$$\begin{aligned} F_d(\theta_r) &= \sum_{n=1}^{\infty} F_{dn}\cos(n\theta_r - \varphi') = F_d(\omega t) \\ &= \sum_{n=1}^{\infty} F_{dn}\cos(n\omega t - \varphi')\,, \\ F_{dn} &= \sqrt{a_n^2 + b_n^2} = \frac{\sqrt{2}I_f n_m}{n\pi}\sqrt{1-\cos n\alpha_r} \\ &= \frac{2I_f n_m}{n\pi}\sin\frac{n\alpha_r}{2}\,, \\ \varphi' &= \arctan\frac{b_n}{a_n} = \frac{n\alpha_r}{2} + n\beta'\,. \end{aligned} \tag{8}$$

Since $0 < \alpha_r < \pi$, according to (8), F_{dn} will be zero when $n > 3$ and $\alpha_r = 2k\pi/n (k = 1, 2, 3, \ldots,$ and n is the harmonic order number), more details are shown in Tab. 1.

When on an ISCF state, ignoring the higher harmonic components and only taking $n = 1$ and $n = 2$ into account, the MMFs are indicated as Fig. 4, where F_{d1} and F_{d2} are the fundamental-frequency component and the 2nd harmonic component of the reverse MMF, respectively, F_C is the composite 1st harmonic component composed by F_1 and F_{d1}, φ_1 is the angle between F_{d1} and the horizontal axis, and φ_2 is the angle between F_{d2} and the horizontal axis. In the presented case, the MMF is

$$\begin{aligned} f(\alpha_m, t) &= F_s\cos\big(\omega t - \alpha_m - \psi - \frac{\pi}{2}\big) + F_r\cos(\omega t - \alpha_m) \\ &\quad - F_{d1}\cos(\omega t - \alpha_m - \varphi_1) - F_{d2}\cos 2(\omega t - \alpha_m - \varphi_2) \\ &= F_C\cos(\omega t - \alpha_m - \beta_1) - F_{d2}\cos 2(\omega t - \alpha_m - \varphi_2) \end{aligned} \tag{9}$$

$$\begin{aligned} F_{d1} &= \frac{\sqrt{2}I_f n_m}{\pi}M_1\,, \\ F_{d2} &= \frac{\sqrt{2}I_f n_m}{2\pi}M_2\,, \\ M_1 &= \sqrt{1-\cos\alpha_r} = \sqrt{2}\sin\frac{\alpha_r}{2}\,, \\ M_2 &= \sqrt{1-\cos(2\alpha_r)} = \sqrt{2}\sin\alpha_r\,, \\ F_C &= \big((F_r - F_s\sin\psi - F_{d1}\cos\varphi_1)^2 + \\ &\qquad (F_s\cos\psi - F_{d1}\sin\varphi_1)^2\big)^{1/2}, \\ \beta_1 &= \operatorname{arctg}\frac{F_s\cos\psi - F_{d1}\sin\varphi_1}{F_r - F_s\sin\psi - F_{d1}\cos\varphi_1}\,. \end{aligned} \tag{10}$$

Then, the MFD under ISCF can be modeled by

$$\begin{aligned} B(\alpha_m, t) = f(\alpha_m, t)\Lambda_0 &= [F_C\cos(\omega t - \alpha_m - \beta_1) \\ &\quad - F_{d2}\cos 2(\omega t - \alpha_m - \varphi_2)]\Lambda_0\,. \end{aligned} \tag{11}$$

For the solution of (11), it is convenient to find out that there are only 1st and 2nd harmonic components existing in the MFD. If considering the higher harmonic components, there should be both odd harmonics and even harmonics existing.

Comparing (4) with (11), it is shown that the amplitude at the fundamental-frequency decreases. Besides, there are second harmonic components generated. It can be seen from (10) and (11) that the amplitude of each harmonic is both affected by the number of the short circuit turns (n_m) which indicates the faulty degree and the angle between the slots (α_r) which indicates the shorted position.

The values of M1 and M2, see (10), will be constant when α_r is unchanged. In this case, along with the increase of n_m, the value of F_{d1} and F_{d2} will be increased, while F_c will be decreased. Hence, as the ISCF develops, the amplitude of the 1st harmonic MFD will be decreased while the second harmonic component will be increased. Further, if taking the higher harmonic components into account, the result will be expanded as that the amplitudes of the odd harmonics will be decreased while the

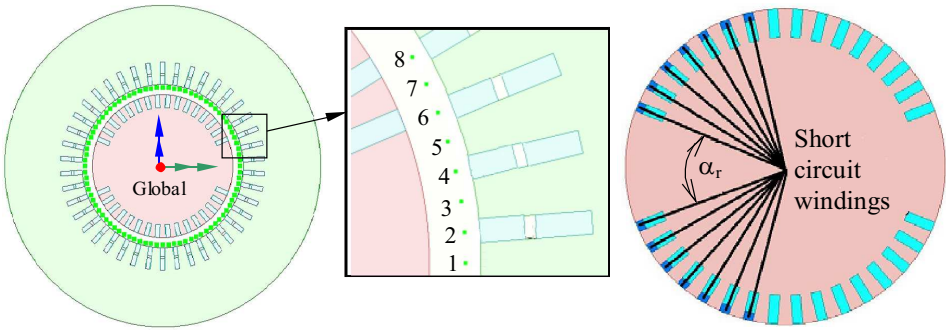

Fig. 5. Simulation model and sampling position set: (a) — faulty model with sampling position set, and (b) — locations of short circuits

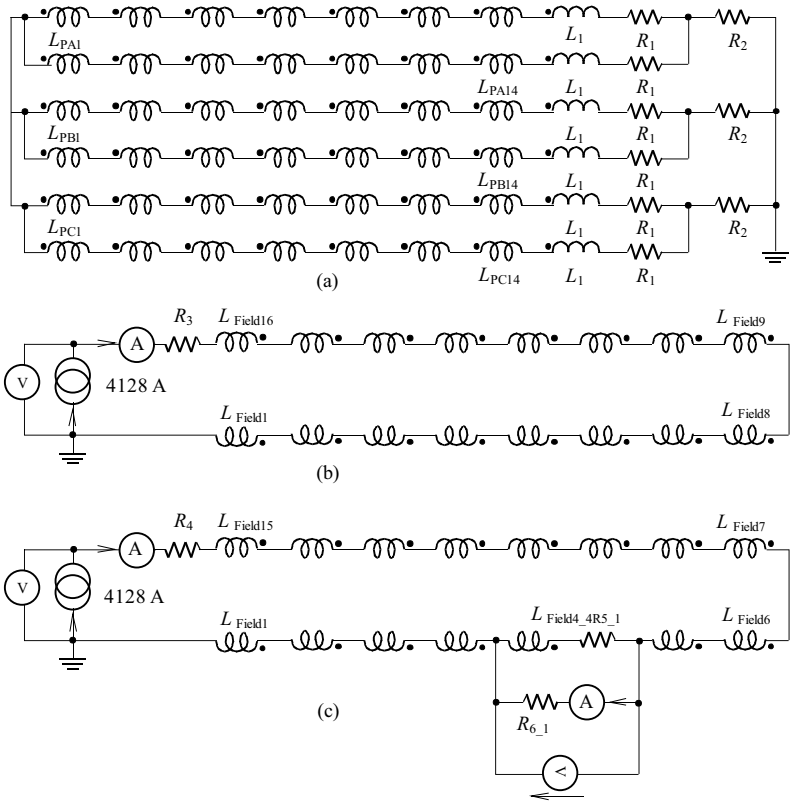

Fig. 6. External circuits of stator and rotor windings: (a) — Circuit of armature windings, (b) — Circuit of excitation windings in normal condition, and (c) — Circuit of excitation windings under ISCF

Table 2. Generator parameters

Rated capacity	666.667 MVA
Rated excitation current	4128 A
Rated speed	3000 r/min
Number of pole pairs	1
Radial air gap length	2 85.5 mm
Pitch-shortening value	0.81
Stator slot number	42
Rotor slot number	16
Number of exciting turns	124

even harmonics will be increased. Besides, according to Fig. 2, it is easy to understand that the increment of n_m will decrease the total passband MFD. In other words, the magnetic field intensity will be decreased.

Keeping n_m constant, with the increment of α_r, M_1 and F_{d1} will be enlarged while F_c will be decreased (see (10)). Differently, M_2 and F_{d2} will be firstly increased and then decreased, with the critical point at $\alpha_r = 90°$. Therefore, as the shorted position shifts away from the magnetic pole (the angle α_r increases), the amplitude of the 2^{nd} harmonic MFD will be firstly increased and then decreased, while the 1^{st} harmonic MFD will be always decreased. As indicated in (9) and (10), it can be found that the developing trend of the 1^{st} harmonic MFD will be always opposite to M_1, while the 2^{nd} harmonic will always follow the variation of M_2. The relation between M_1, M_2 and α_r are shown in Fig. 2 (a) and (b).

Since the increment of F_{d1} will decrease the 1^{st} harmonic amplitude of the MFD, while the rise of F_{d2} will in-

crease the 2nd harmonic MFD, the key problem to determine the changing tendency of the total passband MFD is to distinguish the value of $(F_{d1}-F_{d2})$. It can be confirmed that F_{d1} is larger than F_{d2}, as indicated in

$$F_{d1}-F_{d2}=\frac{2I_f n_m}{\pi}\sin\frac{\alpha_r}{2}-\frac{I_f n_m}{\pi}\sin\alpha_r=$$
$$\frac{I_f n_m}{\pi}\left(2\sin\frac{\alpha_r}{2}-\sin\alpha_r\right)=\frac{I_f n_m}{\pi}\left(2\sin\frac{\alpha_r}{2}-2\sin\frac{\alpha_r}{2}\cos\frac{\alpha_r}{2}\right)$$
$$=\frac{2I_f n_m}{\pi}\sin\frac{\alpha_r}{2}\left(1-\cos\frac{\alpha_r}{2}\right)>0\,. \quad (12)$$

It is obvious that the increment of the angle α_r will both increase the factor $sin(\alpha_r/2)$ and $(1-\cos(\alpha_r/2))$, which means that the decreased value of the 1st harmonic MFD is more than the increased value of the 2nd harmonic MFD. Therefore, as the shorted position shifts away from the magnetic pole, the total passband MFD and the magnetic field intensity will be generally decreased.

Typically, the change of MFD will also be reflected at the stator current. It is easy to deduce that the developing tendency of the stator current will generally follow the developing trend of MFD. Therefore, as the short circuit degree increases, the odd harmonics of the stator current, especially the 1st harmonic will be decreased, while the even harmonics, especially the 2nd harmonic, will be increased. Moreover, as the shorted position shifts away from the magnetic pole, the total stator current and its 1st harmonic will be decreased, while its 2nd harmonic will be firstly increased and then decreased.

3 SIMULATION ANALYSIS

3.1 Model and simulation set

Modeling of ISCF is performed for a QSFN-600-2YHG turbo-generator and its parameters are shown in Tab. 2.

The model is established by the Rmxprt in Ansoft software according to the generator parameters, as indicated in Fig. 5. Since the MFD is a time and space (α_m) dependent function (see (11)), during the simulation, 84 sampling points, which are equally spaced on an air gap circle, are set to extract the performing data. The root mean square (RMS) values of the parameters at these points, such as the harmonic amplitude of the MFD, are calculated to present the general variation condition. Meanwhile, the time-domain curve and its spectrum at Point 1 are also presented to show the detailed partial information. To couple with the FEA model, extra external circuits respectively for the stator windings and the rotor windings are set up, as shown in Fig. 6.

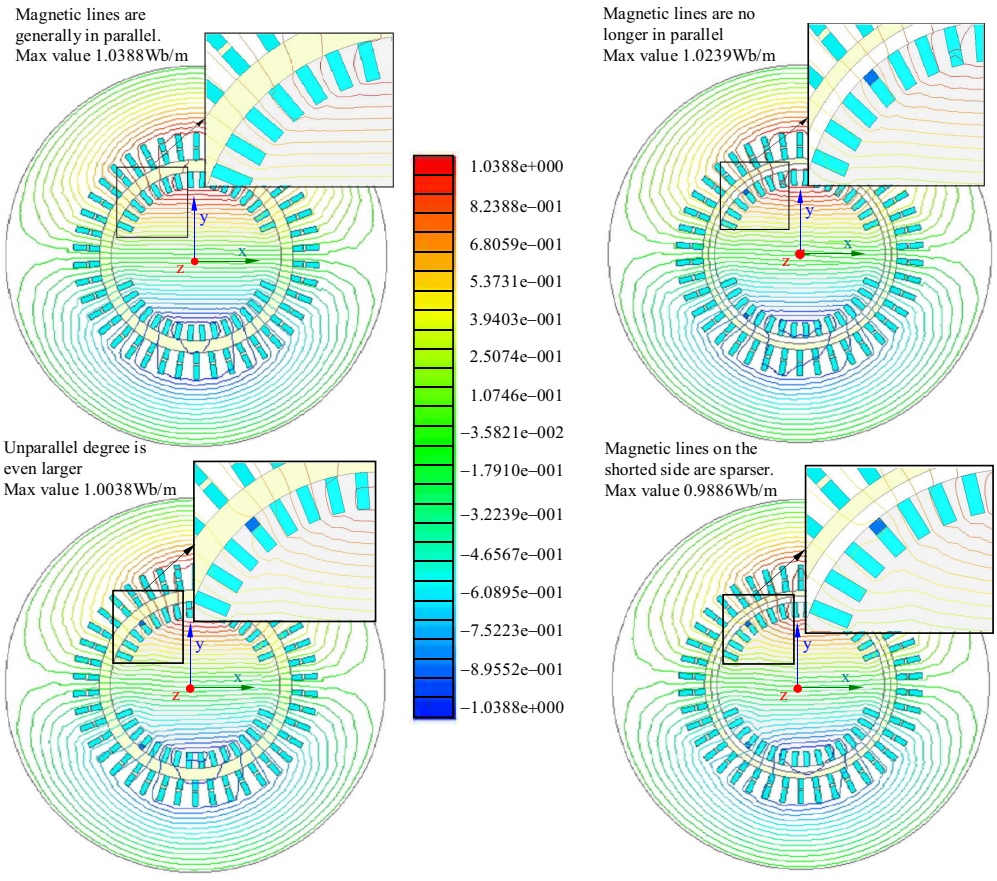

Fig. 7. Distribution of magnetic lines: (a) — normal, (b) — 2 turns shorted in slot 4, (c) —- 4 turns shorted in slot 4, (d) — 6 turns shorted in slot 4

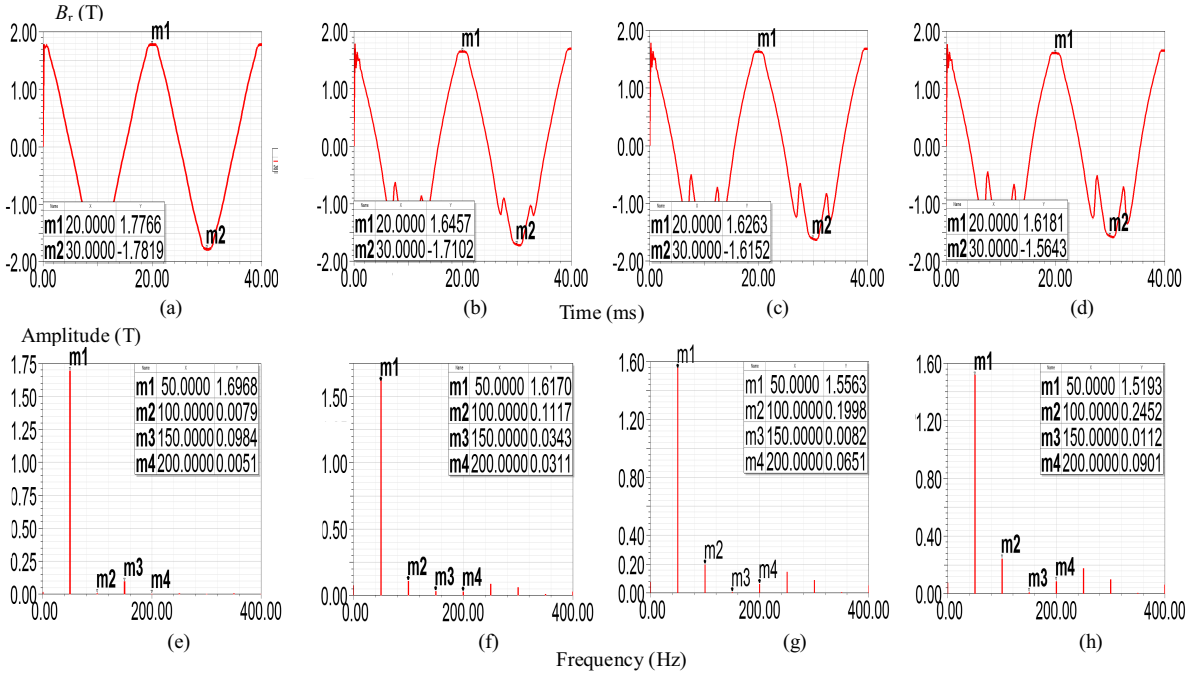

Fig. 8. Time-domain curves and spectrums of MFD at Point 1 respectively for: (a) & (e) — normal condition, (b) & (f) — 2 turns shorted in slot 4, (c) & (g) — 4 turns shorted in slot 4, and (d) & (h) — 6 turns shorted in slot 4

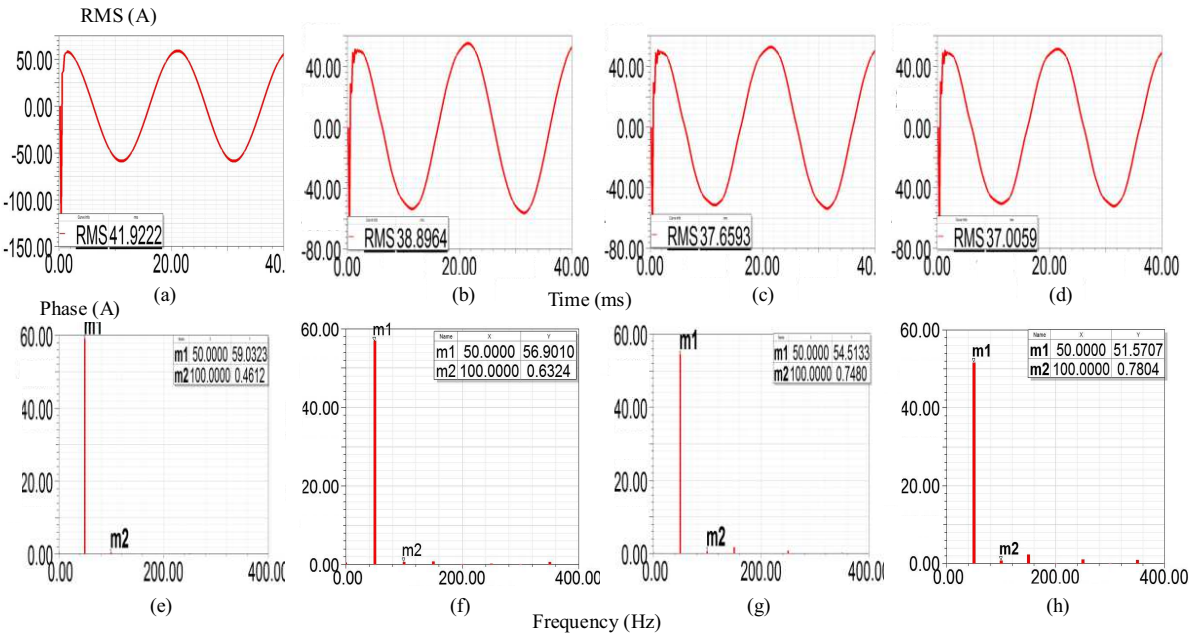

Fig. 9. The RMS values and spectrums of Phase current respectively for: (a) & (e) — normal condition, (b) & (f) — 2 turns shorted in slot 4, (c) & (g) — 4 turns shorted in slot 4, and (d) & (h) — 6 turns shorted in slot 4

3.2 Results and discussion

1) Effect of short circuit degree on MFD

There are respectively 2, 4, and 6 turns shorted in Slot 4, and the distribution of the magnetic flux lines are shown in Fig. 7. The significant parameters, including the RMS peak-to-peak value and the 1st to 4th harmonic amplitudes of the MFD, are shown in Tab. 3, while the time domain curves and their spectrums of Point 1 are shown in Fig. 8. Besides, as a reflection, the detailed variation of the phase current is indicated in Fig. 9 and Tab. 4.

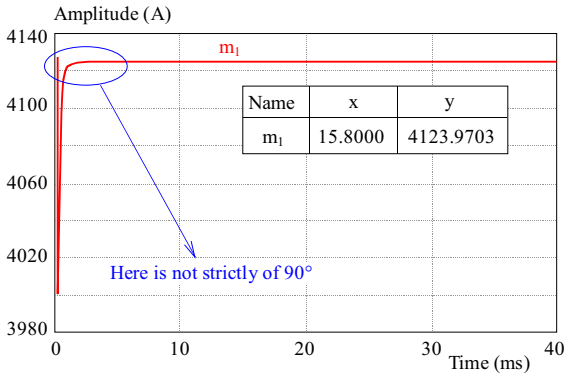

Fig. 10. The exciting current curve

Table 3. RMS values of significant parameters under different conditions

The operating state	The time domain curve of MFD	The amplitude of spectrum of MFD			
	RMS peak-to-peak value(T)	50Hz(T)	100Hz(T)	150Hz(T)	200Hz(T)
Normal condition	3.3759	1.5903	0.0173	0.0959	0.0129
2 turns were shorted in slot4	3.2202	1.4700	0.1657	0.0303	0.0700
4 turns were shorted in slot4	3.1126	1.4172	0.2312	0.0205	0.1022
6 turns were shorted in slot4	3.0560	1.3890	0.2639	0.0206	0.1201

Table 4. Amplitude of Phase A under different conditions

Operating state	Time domain curve of Phase current	Harmonic amplitude of Phase current	
	RMS value (A)	50Hz(A)	100Hz(A)
Normal condition	41.9222	59.0323	0.4612
2 turns shorted in slot4	38.8964	56.9010	0.6324
4 turns shorted in slot4	37.6593	54.5133	0.7480
6 turns shorted in slot4	37.0059	51.5707	0.7804

Table 5. RMS values of significant parameters under different conditions

The operating state	The time domain curve of MFD	The amplitude of spectrum of MFD	
	RMS peak-to-peak value(T)	50Hz(T)	100Hz(T)
Normal condition	3.3759	1.5903	0.0173
4 turns shorted in slot 1	3.2438	1.5324	0.1100
4 turns shorted in slot 2	3.1250	1.4952	0.1642
4 turns shorted in slot 3	3.1161	1.4568	0.2051
4 turns shorted in slot 4	3.1126	1.4172	0.2312
4 turns shorted in slot 5	3.1061	1.3971	0.2047
4 turns shorted in slot 6	3.0247	1.3696	0.1707
4 turns shorted in slot 7	3.0118	1.3451	0.1201

Table 6. Amplitude of Phase A under different conditions

The operating state	The time domain curve of Phase A	The amplitude of spectrum of Phase A	
	The RMS value (A)	50Hz(A)	100Hz(A)
Normal condition	41.9222	59.0323	0.4612
4 turns were shorted in slot 1	40.3807	57.7234	0.5734
4 turns were shorted in slot 2	39.5832	56.9010	0.6324
4 turns were shorted in slot 3	38.6633	55.7720	0.7018
4 turns were shorted in slot 4	37.6593	54.5133	0.7480
4 turns were shorted in slot 5	37.6593	53.6638	0.7531
4 turns were shorted in slot 6	36.9938	52.5818	0.7388
4 turns were shorted in slot 7	36.1005	51.8064	0.7091

Theoretically, there should be no even harmonics in normal condition. However, the simulation result (see Tab. 3) shows that there are actually 2^{nd} and 4^{th} harmonics of tiny values existing. This is mainly caused due to the off-standard square wave of the exciting current at the beginning time, for the step section is not strictly of 90°, as shown in Fig. 10 (the expansion of the standard square wave in Fourier series has only odd harmonics, while off-standard one has also even harmonics).

As presented in Fig. 7 (b)–(d), it is found that as the number of the short circuit turns increases, the magnetic field intensity will be decreased, and the magnetic flux lines will be inclined to the side on which the ampere-turns are larger (the un-shorted side). Comparing (b)–(d) with (a), it is easy to see that the magnetic flux lines inside the rotor are in parallel under normal condition, while they are unparallel and will be sparser on the shorted side in the case of ISCF. The developing tendency of the simulated magnetic distribution follows the previously theoretical analysis. Meanwhile, as shown in Fig. 8, the faulty MFD curves in time domain are no longer a standard sine wave. As the ISCF develops, the curve amplitude and the peak-to-peak value will be decreased, while the partial distortion will be increased. Moreover, as ISCF develops, the odd harmonics (since the values of the higher order harmonics are very tiny, here only the 1^{st} and the 3^{rd} harmonics are noted) will be decreased,

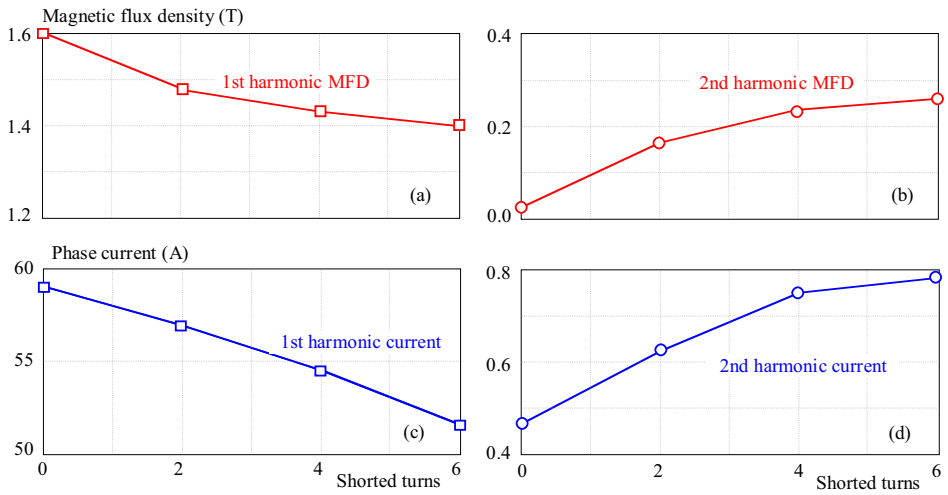

Fig. 11. Developing trend of MFD and the phase current due to different shorted turns: (a) — 1st harmonic MFD, (b) — 2nd harmonic MFD, (c) — 1st harmonic phase current, and (d) — 2nd harmonic phase current

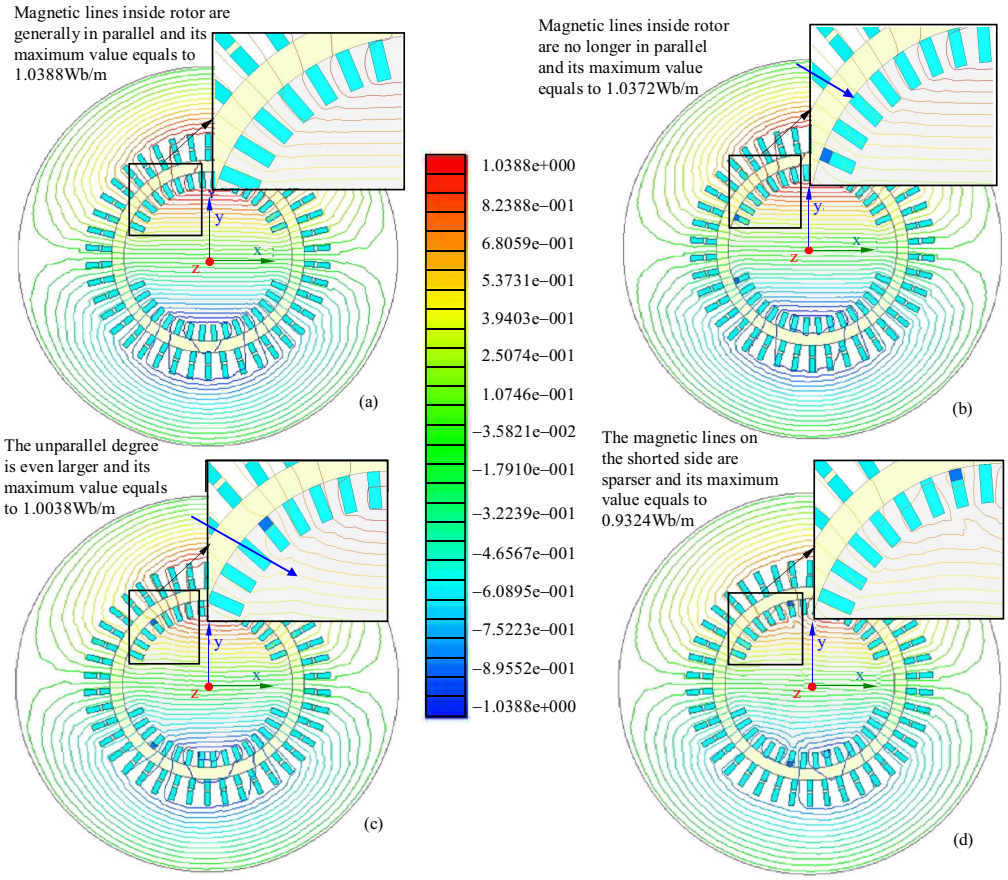

Fig. 12. Distribution of magnetic flux lines respectively for: (a) — normal condition, (b) — 4 turns shorted in slot 1, (c) — 4 turns shorted in slot 4 and (d) — 4 turns shorted in slot 7

while the even harmonics (such as the 2nd and the 4th harmonics) will be increased.

It is easy to get the point from Fig. 9 and Tab. 4 that, comparing with normal condition, the RMS value of the armature current are decreased. Meanwhile, the 1st harmonic is decreased while the 2nd harmonic is increased. The developing tendency of the phase current follows the MFD variations well. To better illustrate the comparison between MFD and the phase current, the developing trend of the 1st and 2nd harmonic respectively for MFD and the phase current are put together, as indicated in Fig. 11.

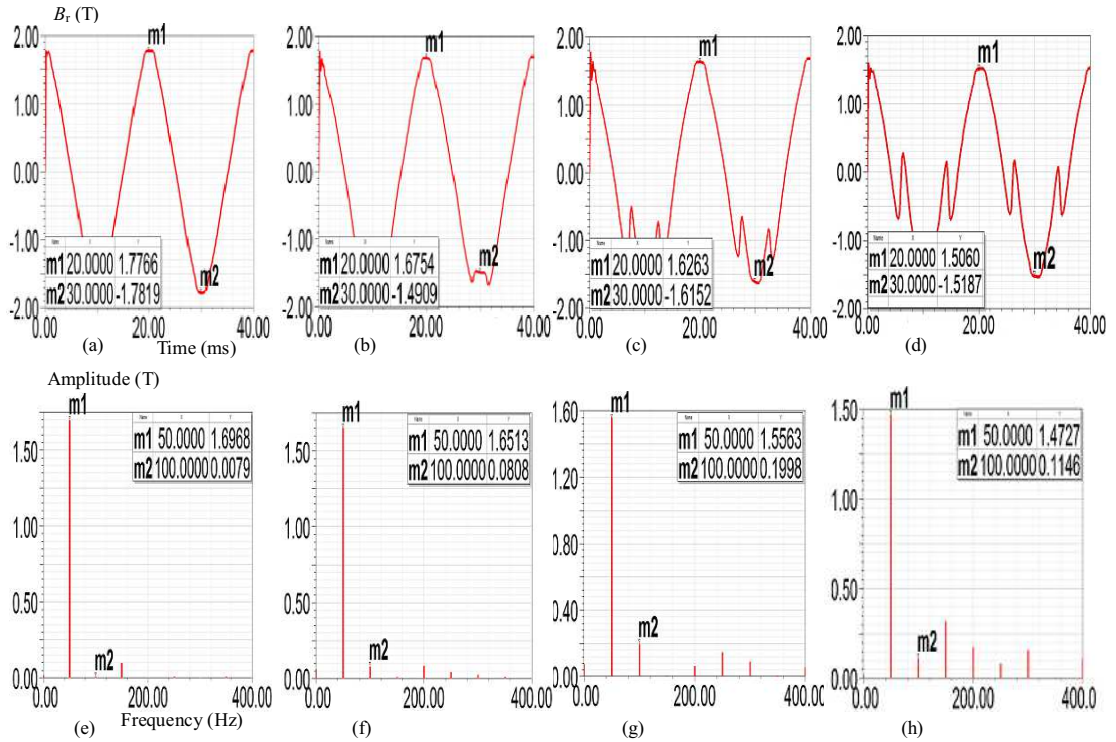

Fig. 13. Time-domain curves and spectrums of Point 1 respectively for: (a) & (e) — normal condition, (b) & (f) — 4 turns shorted in slot 1, (c) & (g) — 4 turns shorted in slot 4, and (d) & (h) — 4 turns shorted in slot 7

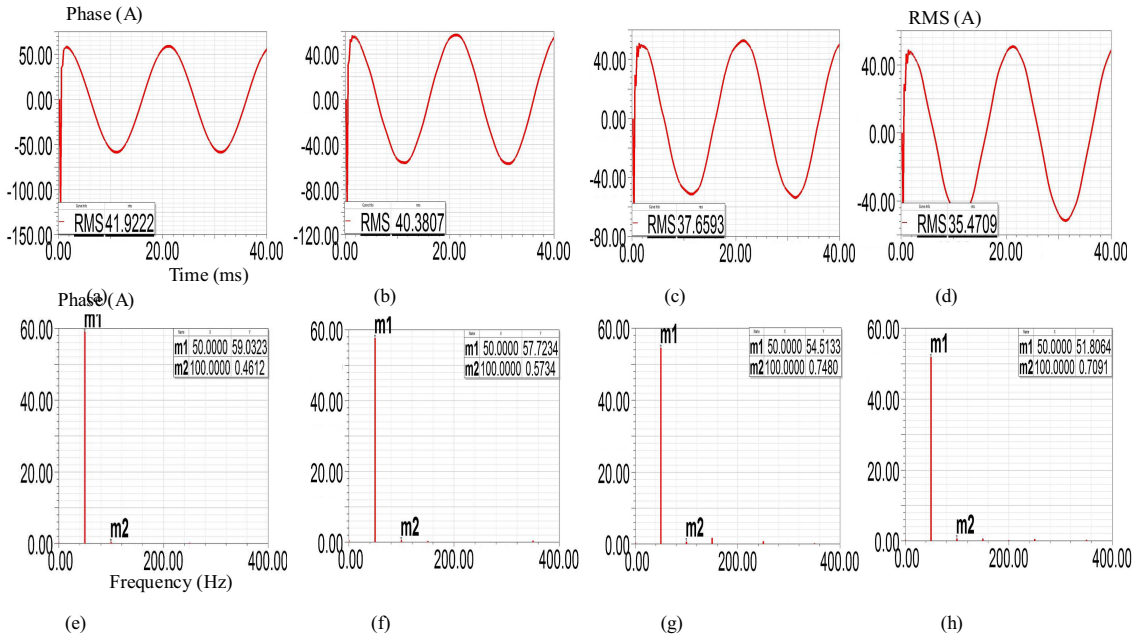

Fig. 14. The RMS values and spectrums of Phase A under different conditions respectively for: (a) & (e) — normal condition, (b) & (f) — 4 turns shorted in slot 1, (c) & (g) — 4 turns shorted in slot 4, and (d) & (h) — 4 turns shorted in slot 7

2) Effect of short circuit location on MFD

There are 4 turns shorted respectively in slot 1 to slot 7 (see Fig. 5). The RMS values of the harmonic amplitudes and the peak-to-peak values of the 84 points are shown in Tab. 5. The distribution conditions of the magnetic flux lines are indicated in Fig. 12, and the time-domain curves and the spectrums of Point 1 are shown in Fig. 13 (due to the limited space, only the cases of 4 turns shorted in slot1, slot 4 and slot 7 are listed), while as a reflection to the MFD the RMS variation of the Phase current is indicated in Fig. 14 and Tab. 6.

As indicated in Fig. 12 and Tab. 5, the increment of α_r will lead to the decrease of the magnetic field intensity. In other words, the short circuit occurs on the location that close to the magnetic pole has a smaller effect on the magnetic field intensity than in other places. In addition, the

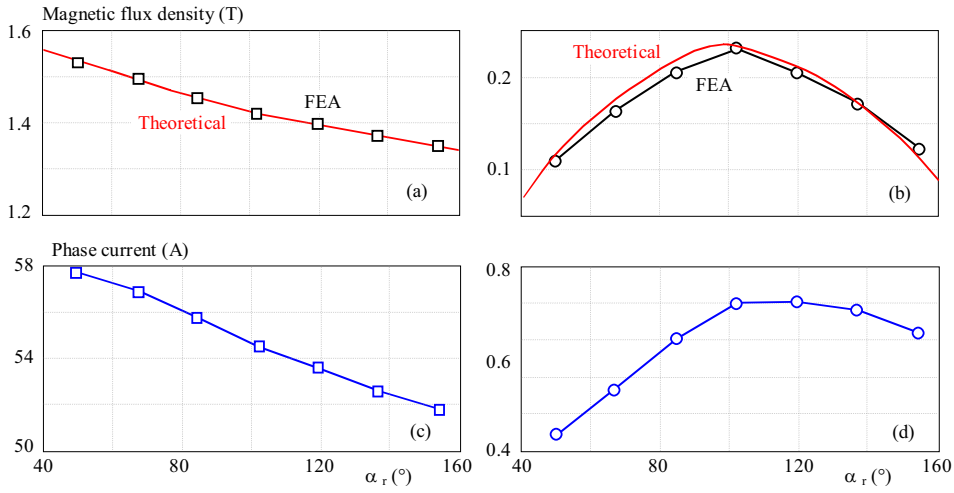

Fig. 15. Comparison between theoretical and simulating results: (a) — 1st harmonic MFD comparison, (b) — 2nd harmonic MFD comparison, (c) — 1st harmonic current of Phase A, and (d) — 2nd harmonic current of Phase A

partial information at Point 1 that presented in Fig. 13 is found to be generally in agreement with the statistic RMS values in Tab. 5. It can be seen that as α_r increases, the 1st harmonic amplitude will be decreased, while the 2nd harmonic amplitude will be firstly increased and then decreased. Meanwhile, the increment of the angle α_r will also intensify the partial distortion degree of the time domain curve. Moreover, as indicated in Tabs. 5 and 6, the 1st harmonic amplitude of MFD and the phase current will have the same decreasing trend as the magnetic field intensity, while the 2nd harmonic amplitudes will both be firstly increased and then decreased. These simulation results follow the previously theoretical analysis well.

4 CONCLUSIONS

This paper presents an analysis and simulation on MFD of turbo-generator under normal condition and ISCF. The effects of the shorted degree and the shorted location on MFD are both taken into account. The study shows that the MFD results can be objectively reflected by the phase current which can be easily obtained on the machine terminal. The primary conclusions drawn from the theoretical analysis and the simulation work are as follows:

1) The distribution of the magnetic flux lines in normal condition is symmetric, and the MFD has only odd harmonics. However, when the ISCF occurs, the distribution of the magnetic flux lines will distort. The magnetic neutral line will shift away from the shorted side, on which the magnetic flux lines are sparser. Besides, there will be even harmonics produced while the RMS of armature current changed.

2) When the faulty position is stable, the development of the short circuit will decrease the odd harmonics (especially the 1st harmonic) but meanwhile increase the even harmonics (especially the 2nd harmonic). As the number of the short circuit turns increases, the magnetic field intensity and the peak-to-peak value will be decreased, and the distortion of the magnetic field will be intensified.

3) When the faulty degree is stable, the increment of the angle α_r, which indicates the angle between the two slots where the interturn short circuit takes place, will generally decrease the magnetic field intensity, the RMS of armature current and the 1st harmonic amplitude of MFD. However, for the 2nd harmonic, the amplitude will be firstly increased and then decreased. The critical point where $\alpha_r = 90°$ is between Slot 3 and Slot 4.

4) The stator phase current follows the variation of MFD and objectively reflects the MFD developing tendency. Therefore, it can be potentially applied in practice to help identify ISCF failure of generator.

In this paper, the significant formulas, which is confirmed by the simulation results, are deduced to indicate the relation between the harmonic amplitude of the MFD and the faulty degree (via n_m, the number of the short circuit turns), and the relation between the MFD harmonic amplitude and the faulty position (via α_r, the angle of the two slots in which the interturn short circuit occurs). Furthermore, the developing trend of the RMS value, the 1st harmonic, and the 2nd harmonic value of the phase current, has been proved to be a objective reflection of MFD. The study work presented in this paper can be probably used as a basis and reference to improve the monitoring level for ISCF.

Acknowledgement

This work is in part supported by the Chinese Fundamental Research Funds for the Central Universities (2015ZD27), the Natural Science Foundation of Hebei Province, China (E2015502013, E2014502052), and the National Natural Science Foundation of China (No. 51307058).

References

[1] SULLA, F. Svensson,—J.—SAMUELSSON, O.: Symmetrical and Unsymmetrical Short-Circuit Current of Squirrel-Cage and Doubly-Fed Induction Generators, Electric Power Systems Research **81** No. 7 (2011), 1610–1618.

[2] KLONTZ, K. W.—MILLER. T. J. E.—McGILP. M. I.—KARMAKER, H.—ZHONG, P.: Short-Circuit Analysis of Permanent-Magnet Generators, IEEE Transactions on Industry Applications **47** No. 4 (2011), 1670–1680.

[3] ALBRIGHT, D. R.: Inter-turn Short-Circuit Detector for Turbine-Generator Rotor Windings, IEEE Transactions on Power Apparatus and Systems **PAS-90** No. 2 (1971), 478–483.

[4] FISER, R.—LAVRIC, H.—BUGEZA, M.—MAKUC, D.: FEM Modeling of Inter-Turn Short-Circuits in Excitation Winding of Turbo-Generator, Przeglad Elektrotechniczny **87** No. 3 (2011), 49–52.

[5] LI, G. J.—HLOUI, S.—OJEDA, J.—HOANG, E.—LECRIVAIN, M.—GABSI. M.—ZHU, Z. Q.: Excitation Winding Short-Circuits in Hybrid Excitation Permanent Magnet Motor, IEEE Transactions on Energy Conversion **29** No. 3 (2014), 567–575.

[6] WAN SHUTING—LI YONGGANG—LI HEMING—TANG GUIJI: The Analysis of Generator Excitation Current Harmonics on Stator and Rotor Winding Fault, IEEE International Symposium on Industrial Electronics, vol. 3, 2006, pp. 2089–2093.

[7] WALLIN, M.—LUNDIN, U.: Dynamic Unbalanced Pull from Field Winding Turn Short Circuits in Hydropower Generators, Electric Power Components and Systems **41** No. 16 (2013), 1672–1685.

[8] YONGGANG, L.—GUOWEI, Z.—YUCAI, W.—HEMING, L.: Impact of rotor inter-turn short-circuit on generator rotor force, Appl. Mechan. Mater **143-144** (2012), 125-131..

[9] LIN WANG—CHEUNG, R. W.—ZHIYUN MA—JIANGJUN RUAN—YING PENG: Finite-Element Analysis of Unbalanced Magnetic Pull in a Large Hydro-Generator under Practical Operations, IEEE Transactions on Magnetics **44** No. 6 (2008), 1558–1561.

[10] RAMIREZ-NINO, J.—PASCACIO. A.: Detecting Interturn Short Circuits in Rotor Windings, Computer Applications in Power, IEEE **14** No. 4 (2001), 39–42.

[11] CAMPBELL, S. R.—KAPLER, J.—SASIC, M.—STONE, G. C.: Detection of Rotor Winding Shorted Turns in Turbine Generators and Hydrogenerators, Cigre 2010 Session, Paris, France, 22-27 August 2010.

[12] BIET, M.: Rotor Faults Diagnosis using Feature Selection and Nearest Neighbors Rule: Application to a Turbogenerator, IEEE Trans. Indust. Electron **60** No. 9 (2013), 4063–4073.

[13] KHEZZARA.—KAIKAAM. Y.—El KAMEL OUMAAMAR, M.—BOUCHERMA, M.—RAZIK, H.: On the Use of Slot Harmonics as a Potential Indicator of Rotor Bar Breakage in the Induction Machine, IEEE Transactions on Industrial Electronics **56** No. 11 (2009), 4592–4605.

[14] QING WU—NANDI, S.: Fast Single-Turn Sensitive Stator Interturn Fault Detection of Induction Machines Based on Positive- and Negative-Sequence Third Harmonic Components of Line Currents, IEEE Transactions on Industry Applications **46** No. 3 (2010), 974–983.

Received 8 December 2015

Yu-Ling He was born in 1984, Fujian Province, China. He received two B.S. degrees respectively in Mechanical Engineering and Electrical Engineering in 2007, the MS degree in Mechatronics Engineering in 2009, and the PhD degree in Power Machinery & Engineering in 2012, all from North China Electric Power University, China. His main research interest is condition monitoring and fault diagnosis on large power equipments.

Meng-Qiang Ke was born in 1989, Fujian Province, China. He received the BS degree in Mechanical Engineering in 2013, and the MS degree in Mechatronics Engineering in 2016, both from North China Electric Power University, China. His main research interest is fault diagnosis on rotary machine.

Gui-Ji Tang was born in 1962, Shandong Province, China. He received the BS degree in Mechanical Engineering, the MS degree in Power Plant Engineering, and the PhD degree in Thermal Engineering, in 1983, 1991, and 1999, respectively, all from North China Electric Power University, China. His main research interests include testing technology, vibration monitoring and control, fault diagnosis on rotary machine.

Hong-Chun Jiang was born in 1982, Hebei Province, China. She received the BS degree in Mechanical Engineering, the MS degree in Mechanical Design and Theory, in 2005 and 2008, respectively, both from North China Electric Power University, China. Now she is working toward the PhD degree in Power machinery and Engineering at North China Electric Power University. Her main research interest is condition monitoring and fault diagnosis on large generators.

Xing-Hua Yuan was born in 1982, Hebei Province, China. She received the BS degree in Mechanical Engineering, the MS degree in Mechatronics Engineering, in 2005 and 2008, respectively, both from North China Electric Power University, China. Now she is working toward the PhD degree in Power machinery and Engineering at North China Electric Power University. Her main research interest is condition monitoring and fault diagnosis on large generators.